ECCOMAS

Proceedia

COMPUTATION OF THE RESPONSE OF DAMAGED RAILWAY TRACKS SUBJECTED TO CONSTANT MOVING LOADS: NUMERICAL RESULTS OBTAINED WITH THE WAVE FINITE ELEMENT METHOD AND ANALYTICAL RESULTS.

Benjamin Claudet[1], Denis Duhamel[1], Gilles Foret[1], Tien Hoang[1], Francis Sabatier[2], Bertrand Findinier[2], and Hervé Lenglin[2]

[1]Navier Laboratory, UMR8205
École des Ponts ParisTech
Champs-sur-Marne, France
e-mail: {benjamin.claudet,denis.duhamel,gilles.foret,tien.hoang}@enpc.fr

[2] GETLINK
Coquelles, France
e-mail: {francis.sabatier,bertrand.findinier,herve.lenglin}@eurotunnel.com

Abstract. *Railway tracks are subjected to heavy repeated loads due to the train traffic. These loads can damage the track and especially its supports. To compute the behavior of railway tracks, many authors used a periodicity hypothesis, which is broken by the presence of a damaged zone. Researchers proposed different analytical or numerical methods to compute the dynamics of such structures. Analytical methods permit low numerical cost computations of the track dynamics, but are limited to very simple representations of the track, whereas numerical methods allow the use of much more detailed representations of the track but with higher numerical cost.*

In most regions, railway tracks can be modeled as periodic structures. Several methods take advantage of this periodicity to limit the numerical cost for the computation of the track dynamics. Among these methods, the Wave Finite Element (WFE) method was initially created to compute free vibrations in periodic structures. This method was improved to compute the dynamic response of periodic structures subjected to any kind of loads. In recent development, the authors adapted the WFE method to compute the response of structures composed of two semi infinite periodic zones linked by a central zone with different mechanical properties.

In this paper, the results obtained with an analytical method will be compared to results obtained with the WFE method for the computation of the dynamic responses of different ballastless railway tracks such as healthy and damaged tracks. In these computations, the tracks will be subjected to constant moving loads representing the load applied by a train wheel. In the WFE results, the rail, the supports, and the supporting concrete slabs are represented with a three-dimensional model. A special focus will be made on the state of stress of the different

Keywords: Wave Finite Element Method, Railway, Dynamics, Moving loads, Transition zones, Damaged and reinforced tracks.

materials which constitute the tracks. A failure criterion will be computed at components scale for the different tracks simulated. This criterion can then be used to compute the likeliness of long-term fatigue of the track components.

1 Introduction

During their exploitation, railway tracks are subjected to heavy repeated loads leading to fatigue damages. Numerical simulations can be conducted to understand the mechanical behavior of railway tracks and to anticipate their degradation. To limit the cost of this computation, several authors modeled railway tracks as periodic structures. With this periodicity hypothesis, authors proposed both analytical [1–4] and numerical [5–8] models for computing railway tracks dynamics.

In many cases the track contains portions with different mechanical properties, which breaks its periodicity. These different mechanical properties can come from transition between portions with different natures – like ballasted to ballastless tracks – but also from local damage or reinforcement of the track. To simulate such tracks, one have to use tools which takes into account the periodicity breakage.

In 2017, Hoang *et al.* [9] proposed an analytical model to compute the response of a railway track resting on a non-uniform foundation subjected to constant moving loads. In this model, the rail is represented by a Euler beam and its supports by mass-spring-dampers systems. This model was then reused by Tran *et al.* [10]. Claudet *et al.* [11] developed a similar model representing the rail by a Timoshenko beam.

In recent years, several authors proposed numerical models of railway tracks containing periodicity breaks [5, 12–16]. Among them, Claudet *et al.* [16], in COMDYN 2021, proposed a method to compute the mechanical response of structures constituted of two semi-infinite periodic structures linked by a central part and subjected to moving or fixed loads. To do so, the authors combined the Wave Finite Element (WFE) method – for the periodic zones – and classical Finite Element Method (FEM) – for the central zone. In this method, the WFE method enables taking into account the infinite nature of the geometry. In the presented example, this method was used to simulate a damaged railway track using a one dimensional model.

In the present article, the mechanical behavior of tracks containing one damaged support is studied. A special focus is done on evaluating the level of stresses in the tracks' components depending on the level of degradation of the damaged support. For this study, analytical results will be compared to numerical ones. The analytical results are obtained with the method proposed by Hoang *et al.* [9] and improved by Claudet *et al.* [11]. The numerical model uses the WFE method proposed by Claudet *et al* [16] in COMDYN 2021. These numerical results uses a fine three-dimensional model of the damaged tracks.

2 Methods used

This section briefly describes the two methods used in the present article to compute the dynamical response of damaged railway tracks. In the considered tracks, each support is constituted of a reinforced concrete block linked to the rail and the underlying concrete slab by two elastic stages. The first elastic stage is situated between the rail and the concrete block and is called rail pad. The second one, situated between the concrete bloc and the slab, is called undersleeper pad.

2.1 Analytical method

In the analytical method proposed by Claudet *et al.* [11], in healthy zone, the track is represented by a periodically supported Timoshenko beam. The beam represents the rail and the supports are modeled by mass-springs-dampers systems (see figure 1).

Claudet *et al.* supposed the track contains a finite number of supports with varying spacings
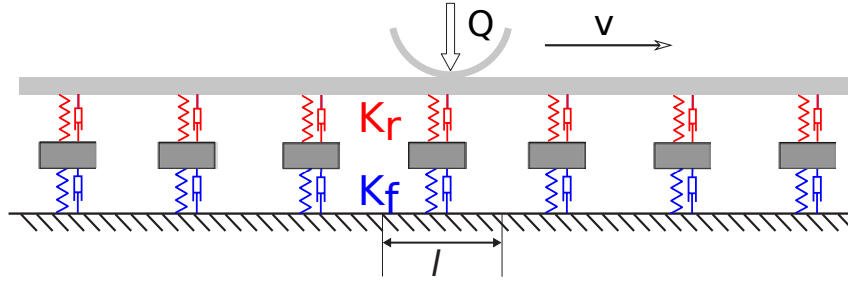
Benjamin Claudet, Denis Duhamel, Gilles Foret, Tien Hoang, Francis Sabatier, and Hervé
Lenglin

Figure 1: Periodically supported beam model.

or dynamic stiffnesses. This structure is subjected to constant loads Q_j situated at $x = -D_j$ at $t = 0$. These loads are moving at a constant speed v. To compute the response of this structure, the authors considered an auxiliary problem of the response of a beam resting on a repetition of a set of m supports. The length of the structure's pattern is noted L. Figure 2 gives a representation of the true problem and the auxiliary problem (with $m = 5$) for a track containing one damaged support.
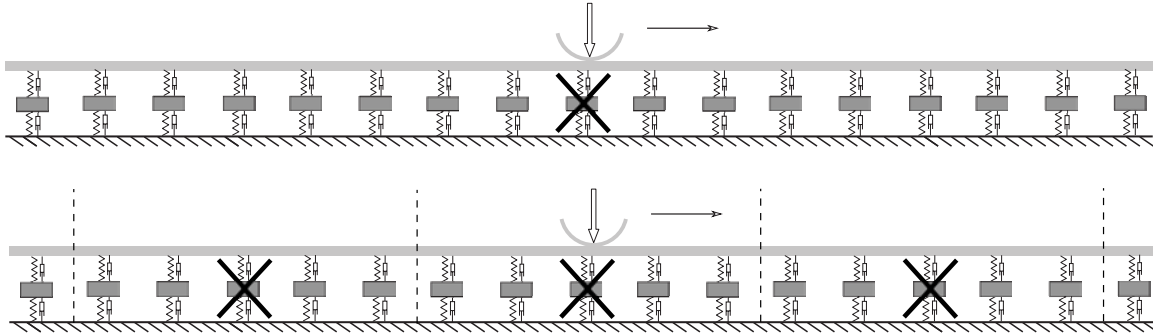

Figure 2: Railway track containing one damaged support. True problem (top), auxiliary problem with $m = 5$ (bottom).

The authors proved that, at a given frequency ω and a given position x, denoting $\hat{R}_p(\omega)$ the force applied by the support p, the rail deflection $\hat{w}$ is given by:

$$\hat{w}(x,\omega) = \sum_{p=0}^{m-1} \hat{R}_p(\omega) e^{i\omega \frac{pl-x}{v}} \eta(pl - x, \omega) - \eta(0,\omega)\mathcal{Q}(\omega)e^{-i\frac{\omega x}{v}} \tag{1}$$

Where,

$$\eta(x,\omega) = \frac{e^{i\frac{\omega x}{v}}}{2EI\left(\lambda_1^2 + \lambda_2^2\right)}\left[\frac{C_1}{\lambda_1} \frac{\sin\lambda_1(L-x) + e^{-i\frac{\omega L}{v}}\sin\lambda_1 x}{\cos L\lambda_1 - \cos\frac{\omega L}{v}} \right.$$
$$\left. - \frac{C_2}{\lambda_2} \frac{\sinh\lambda_2(L-x) + e^{-i\frac{\omega L}{v}}\sinh\lambda_2 x}{\cosh L\lambda_2 - \cos\frac{\omega L}{v}} \right]$$

$$\mathcal{Q}(\omega) = \frac{\widetilde{p}_0 L}{v}\eta(0,\omega)^{-1}\sum_{j=1}^{K} Q_j e^{-i\omega\frac{D_j}{v}}$$

With,

$$C_{1,2} = 1 - \frac{\rho I \omega^2 \mp EI\lambda_{1,2}^2}{\kappa S G}$$

$$\lambda_{1,2}^2 = \sqrt{\frac{\omega^4}{4}\left(\frac{\rho I}{EI} - \frac{\rho S}{\kappa S G}\right)^2 + \frac{\rho S \omega^2}{EI}} \pm \frac{\omega^2}{2}\left(\frac{\rho I}{EI} + \frac{\rho S}{\kappa S G}\right)$$

$$\widetilde{p}_0 L = \frac{\kappa S G - \rho I \omega^2 + EI\frac{\omega^2}{v^2}}{\kappa S G \left(EI\frac{\omega^4}{v^4} - \rho S \omega^2\right) - \rho S I \left(\kappa G + E - \rho v^2\right)\frac{\omega^4}{v^2}}$$

With I the beam's inertia, G its shear modulus and S its section, κ its Timoshenko shear coefficient and E the Young modulus of the beam's material, ρ its density.

This leads to the following system:

$$\begin{pmatrix} \eta_0 & \eta_1 & \cdots & \eta_{m-1} \\ \eta_{m-1} & \eta_0 & \cdots & \eta_{m-2} \\ \vdots & \vdots & \ddots & \vdots \\ \eta_1 & \eta_2 & \cdots & \eta_0 \end{pmatrix} \begin{pmatrix} \hat{\mathbf{R}}_0 \\ \hat{\mathbf{R}}_1 \\ \vdots \\ \hat{\mathbf{R}}_{m-1} \end{pmatrix} = \eta_0 \mathcal{Q} \begin{pmatrix} 1 \\ 1 \\ \vdots \\ 1 \end{pmatrix} + \begin{pmatrix} \hat{\mathbf{w}}_0 \\ \hat{\mathbf{w}}_1 \\ \vdots \\ \hat{\mathbf{w}}_{m-1} \end{pmatrix} \tag{2}$$

Which can be rewritten in the following matricial form:

$$\underline{\underline{\mathbf{C}}}\,\hat{\underline{\mathbf{R}}} = \eta_0 \mathcal{Q}\underline{\mathbf{1}} + \hat{\underline{\mathbf{w}}} \tag{3}$$

The problem is then closed using the dynamic stiffness $k_p(\omega)$ of each support of the pattern, giving: $-k_p(\omega)\hat{w}(x_p, \omega) = \hat{R}_p(\omega)$. Using $\underline{\underline{\mathbf{D}}} = -diag(1/k_0, \ldots, 1/k_{m-1})$, one can write:

$$\hat{\underline{\mathbf{R}}} = \mathcal{Q}\underline{\underline{\mathbf{A}}}^{-1}\underline{\mathbf{1}} \tag{4}$$

Where $\underline{\underline{\mathbf{A}}} = \eta_0^{-1}\left(\underline{\underline{\mathbf{C}}} + \underline{\underline{\mathbf{D}}}\right)$.

To solve the auxiliary problem, one can directly use Eq. (4) or the iterative procedure presented in [11]. It is considered that, if m (respectively L) is large enough, then, the solution on one pattern in the auxiliary problem is close to the solution on the same m supports in the real problem.

2.2 Numerical method

Being based on a very simplified representation of the track, the previous model can not give access to stresses and strains at a fine scale. In this aim, in the present article, the numerical method proposed by Claudet *et al.* [16] is used to compute the mechanical response of railway transition zones. In this method, the structure is divided into two semi-infinite periodic zones – called right zone and left zone – and a central finite zone with no special property – called transition zone. The obtained geometry is represented in Figure 3.

To compute the mechanical behavior of the obtained structure, the authors combined the Wave Finite Element (WFE) method in the periodic zones with a Finite Element dynamic equilibrium relationship in the transition zone.

2.2.1 The Wave Finite Element (WFE) method

The WFE method consists in reducing the computation of the mechanical behavior of a periodic structure to a much smaller wave problem at one boundary of one of its patterns. The main steps of this method are described in the following.

Benjamin Claudet, Denis Duhamel, Gilles Foret, Tien Hoang, Francis Sabatier, Bertrand Findinier, and Hervé Lenglin
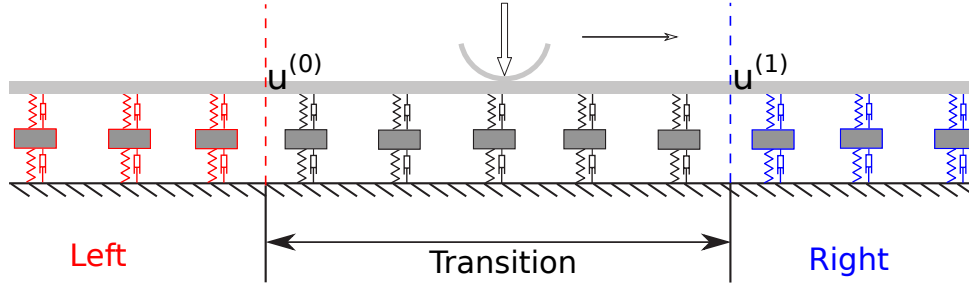

Figure 3: Transition zone between two semi-infinite periodic railway tracks.

In the frequency domain, using the Finite Element Method, the dynamic equilibrium of one pattern can be written. Denoting $\underline{\mathbf{q}}^{(n)}$ the degrees of freedom of the pattern, $\underline{\mathbf{F}}^{(n)}$ the external forces applied on this pattern and $\underline{\underline{\mathbf{D}}}$ its dynamic stiffness matrix, the following equation is obtained:

$$
\begin{bmatrix}
\underline{\underline{\tilde{\mathbf{D}}}}_{II} & \underline{\underline{\tilde{\mathbf{D}}}}_{IL} & \underline{\underline{\tilde{\mathbf{D}}}}_{IR} \\
\underline{\underline{\tilde{\mathbf{D}}}}_{LI} & \underline{\underline{\tilde{\mathbf{D}}}}_{LL} & \underline{\underline{\tilde{\mathbf{D}}}}_{LR} \\
\underline{\underline{\mathbf{D}}}_{RI} & \underline{\underline{\mathbf{D}}}_{RL} & \underline{\underline{\mathbf{D}}}_{RR}
\end{bmatrix}
\begin{bmatrix}
\underline{\mathbf{q}}_I \\
\underline{\mathbf{q}}_L \\
\underline{\mathbf{q}}_R
\end{bmatrix}
=
\begin{bmatrix}
\underline{\mathbf{F}}_I \\
\underline{\mathbf{F}}_L \\
\underline{\mathbf{F}}_R
\end{bmatrix}
\tag{5}
$$

Where the subscripts $_I$, $_L$ and $_R$ respectively stand for inner nodes, left boundary and right boundary nodes.

In the WFE method this equation is transformed into the following propagation equation:

$$
\underline{\mathbf{u}}^{(n+1)} = \underline{\underline{\mathbf{S}}}\,\underline{\mathbf{u}}^{(n)} + \underline{\mathbf{b}}^{(n)}
\tag{6}
$$

Where

$$
\underline{\mathbf{u}}^{(n)} =
\begin{bmatrix}
\underline{\mathbf{q}}_L^{(n)} \\
-\underline{\mathbf{F}}_L^{(n)}
\end{bmatrix}, \quad
\underline{\mathbf{b}}^{(n)} =
\begin{bmatrix}
\underline{\underline{\mathbf{D}}}_{qI}\,\underline{\mathbf{F}}_I^{(n)} \\
\underline{\underline{\mathbf{D}}}_{fI}\,\underline{\mathbf{F}}_I^{(n)} - \underline{\mathbf{F}}_{\partial R}^{(n)}
\end{bmatrix}
$$

$\underline{\underline{\mathbf{S}}}$, $\underline{\underline{\mathbf{D}}}_{qI}$, $\underline{\underline{\mathbf{D}}}_{FI}$ and $\underline{\mathbf{F}}_{\partial R}^{(n)}$ are defined in the works of Hoang *et al.* [17] or Claudet *et al.* [8, 16].

Making use of the propagation equation (6) to compute the mechanical response of a periodic structure, power of $\underline{\underline{\mathbf{S}}}$ matrix appears. To compute the power of $\underline{\underline{\mathbf{S}}}$ matrix, authors compute the eigenvectors of $\underline{\underline{\mathbf{S}}}$. They usually separate eigenvectors $\left\{\underline{\phi}_j\right\}$ corresponding to eigenvalues $\{\mu_j\}$ whose modulus are smaller than 1 and eigenvectors $\left\{\underline{\phi}_j^\star\right\}$ corresponding to eigenvalues $\{\mu_j^\star\}$ whose modulus are greater than 1.

Then the basis $\left\{\underline{\underline{\boldsymbol{\Phi}}}\,\underline{\underline{\boldsymbol{\Phi}}}^\star\right\}$ is defined as: $\underline{\underline{\boldsymbol{\Phi}}} = [\underline{\phi}_1 ... \underline{\phi}_n]$ and $\underline{\underline{\boldsymbol{\Phi}}}^\star = [\underline{\phi}_1^\star ... \underline{\phi}_n^\star]$. Using the subscript "$_q$" (respectively "$_F$") for the components corresponding to the degrees of freedom (DoF) (resp. the loads), leads to Eq. (7).

$$
\underline{\underline{\boldsymbol{\Phi}}} =
\begin{bmatrix}
\underline{\underline{\boldsymbol{\Phi}}}_q \\
\underline{\underline{\boldsymbol{\Phi}}}_F
\end{bmatrix}
\quad
\underline{\underline{\boldsymbol{\Phi}}}^\star =
\begin{bmatrix}
\underline{\underline{\boldsymbol{\Phi}}}_q^\star \\
\underline{\underline{\boldsymbol{\Phi}}}_F^\star
\end{bmatrix}
\tag{7}
$$

Using the same sign convention as in [6, 8, 16], $\mathbf{u}^{(n)}$ and $\mathbf{b}^{(n)}$ can be written in this wave basis:

$$
\begin{aligned}
\underline{\mathbf{u}}^{(n)} &= \underline{\underline{\boldsymbol{\Phi}}}\,\underline{\mathbf{Q}}^{(n)} - \underline{\underline{\boldsymbol{\Phi}}}^\star\,\underline{\mathbf{Q}}^{\star(n)} \\
\underline{\mathbf{b}}^{(n)} &= \underline{\underline{\boldsymbol{\Phi}}}\,\underline{\mathbf{Q}}_E^{(n)} - \underline{\underline{\boldsymbol{\Phi}}}^\star\,\underline{\mathbf{Q}}_E^{\star(n)}
\end{aligned}
\tag{8}
$$

With this notations, Hoang *et al.* [6] proved:

$$
\begin{aligned}
\underline{\mathbf{Q}}_E^{(k)} &= \left[\left(\underline{\underline{\boldsymbol{\mu}}} \, \underline{\underline{\boldsymbol{\Phi}}}_q^{\star T} \, \underline{\underline{\mathbf{D}}}_{LI} + \underline{\underline{\boldsymbol{\Phi}}}_q^{\star T} \, \underline{\underline{\mathbf{D}}}_{RI} \right) \underline{\mathbf{F}}_I^{(k)} - \underline{\underline{\boldsymbol{\Phi}}}_q^{\star T} \, \underline{\mathbf{F}}_{\partial R}^{(k)} \right] \\
\underline{\mathbf{Q}}_E^{\star (k)} &= \left[\left(\underline{\underline{\boldsymbol{\mu}}}^{\star} \, \underline{\underline{\boldsymbol{\Phi}}}_q^{T} \, \underline{\underline{\mathbf{D}}}_{LI} + \underline{\underline{\boldsymbol{\Phi}}}_q^{T} \, \underline{\underline{\mathbf{D}}}_{RI} \right) \underline{\mathbf{F}}_I^{(k)} - \underline{\underline{\boldsymbol{\Phi}}}_q^{T} \, \underline{\mathbf{F}}_{\partial R}^{(k)} \right]
\end{aligned}
\tag{9}
$$

2.2.2 Problem closure

In the previous paragraph, the basic WFE equations were reminded. These equations allow to reduce the mechanical behavior of a periodic structure to a wave problem at one of its boundaries. To close the problem, Claudet *et al.* used the equilibrium relationship of the transition zone. Using the same notations as before, this equilibrium relationship of this zone can be written:

$$
\underline{\underline{\tilde{\mathbf{D}}}}_T \begin{bmatrix} \underline{\mathbf{q}}_I \\ \underline{\mathbf{q}}_L \\ \underline{\mathbf{q}}_R \end{bmatrix} = \begin{bmatrix} \underline{\mathbf{F}}_I \\ \underline{\mathbf{F}}_L \\ \underline{\mathbf{F}}_R \end{bmatrix}
\tag{10}
$$

Lets denote (0) the left boundary of the transition zone and (1) its right boundary – see Fig. 3. Then, denoting with "$_R$" subscript the right zone and "$_L$" subscript the left zone, the following propagation equations are obtained:

$$
\begin{cases}
\forall n \geqslant 1, \ \underline{\mathbf{u}}_R^{(n+1)} = \underline{\underline{\mathbf{S}}}_R \, \underline{\mathbf{u}}^{(n)} + \underline{\mathbf{b}}^{(n)} \\
\forall n \leqslant 0, \ \underline{\mathbf{u}}_L^{(n-1)} = \underline{\underline{\mathbf{S}}}_L^{-1} \, \underline{\mathbf{u}}^{(n)} - \underline{\underline{\mathbf{S}}}_L^{-1} \, \underline{\mathbf{b}}^{(n-1)}
\end{cases}
\tag{11}
$$

Writing,

$$
\begin{aligned}
\underline{\mathbf{u}}^{(0)} &= \underline{\underline{\boldsymbol{\Phi}}}_L \, \underline{\mathbf{Q}}_L - \underline{\underline{\boldsymbol{\Phi}}}_L^{\star} \, \underline{\mathbf{Q}}_L^{\star} \\
\underline{\mathbf{u}}^{(1)} &= \underline{\underline{\boldsymbol{\Phi}}}_R \, \underline{\mathbf{Q}}_R - \underline{\underline{\boldsymbol{\Phi}}}_R^{\star} \, \underline{\mathbf{Q}}_R^{\star}
\end{aligned}
\tag{12}
$$

Claudet *et al.* proved that the dynamics of the structure is ruled by Eq. (13):

$$
\left(\underline{\underline{\tilde{\mathbf{D}}}}_T \, \underline{\underline{\mathbb{C}}}_q - \underline{\underline{\mathbb{C}}}_F \right) \underline{\tilde{\mathbf{q}}} = \underline{\tilde{\mathbf{F}}}
\tag{13}
$$

Where,

$$
\underline{\tilde{\mathbf{q}}} = \begin{bmatrix} \underline{\mathbf{q}}_I \\ \underline{\mathbf{Q}}_L^{\star} \\ \underline{\mathbf{Q}}_R \end{bmatrix}, \quad
\underline{\underline{\mathbb{C}}}_q = \begin{bmatrix} \underline{\underline{\mathbf{I}}} & \underline{\underline{\mathbf{0}}} & \underline{\underline{\mathbf{0}}} \\ \underline{\underline{\mathbf{0}}} & -\underline{\underline{\boldsymbol{\Phi}}}_{L,q}^{\star} & \underline{\underline{\mathbf{0}}} \\ \underline{\underline{\mathbf{0}}} & \underline{\underline{\mathbf{0}}} & \underline{\underline{\boldsymbol{\Phi}}}_{R,q} \end{bmatrix}, \quad
\underline{\underline{\mathbb{C}}}_F = \begin{bmatrix} \underline{\underline{\mathbf{0}}} & \underline{\underline{\mathbf{0}}} & \underline{\underline{\mathbf{0}}} \\ \underline{\underline{\mathbf{0}}} & \underline{\underline{\boldsymbol{\Phi}}}_{L,F}^{\star} & \underline{\underline{\mathbf{0}}} \\ \underline{\underline{\mathbf{0}}} & \underline{\underline{\mathbf{0}}} & \underline{\underline{\boldsymbol{\Phi}}}_{R,F} \end{bmatrix}
$$

$$
\underline{\tilde{\mathbf{F}}} = \begin{bmatrix} \underline{\mathbf{F}}_I \\ -\underline{\underline{\boldsymbol{\Phi}}}_{L,F} \sum_{k=1}^{\infty} \underline{\underline{\boldsymbol{\mu}}}_L^{k-1} \, \underline{\mathbf{Q}}_E^{(-k)} \\ \underline{\mathbf{F}}_{\partial R} + \underline{\underline{\boldsymbol{\Phi}}}_{R,F}^{\star} \sum_{k=1}^{\infty} \underline{\underline{\boldsymbol{\mu}}}_R^{k} \, \underline{\mathbf{Q}}_E^{\star (k)} \end{bmatrix} - \underline{\underline{\tilde{\mathbf{D}}}}_T \begin{bmatrix} \underline{\mathbf{0}} \\ \underline{\underline{\boldsymbol{\Phi}}}_{L,q} \sum_{k=1}^{\infty} \underline{\underline{\boldsymbol{\mu}}}_L^{k-1} \, \underline{\mathbf{Q}}_E^{(-k)} \\ \underline{\underline{\boldsymbol{\Phi}}}_{R,q}^{\star} \sum_{k=1}^{\infty} \underline{\underline{\boldsymbol{\mu}}}_R^{k} \, \underline{\mathbf{Q}}_E^{\star (k)} \end{bmatrix}
\tag{14}
$$

In this equation, vector $\underline{\tilde{\mathbf{q}}}$ contains the unknown of the problem. For known loads, the series $\sum_{k=1}^{\infty} \underline{\underline{\boldsymbol{\mu}}}_L^{k-1} \, \underline{\mathbf{Q}}_E^{(-k)}$ and $\sum_{k=1}^{\infty} \underline{\underline{\boldsymbol{\mu}}}_R^{k} \, \underline{\mathbf{Q}}_E^{\star (k)}$ can be computed using Eq. (9).

3 Results

In this section, the previous models are applied to the computation of the dynamic responses of ballastless railway tracks containing a single damaged support.

To simplify interpretation and the comparison between the two models, we assumed that the structure is subjected to a single constant load $Q = 100\,\text{kN}$ moving at a constant speed v. Due to the support degradation, the neighboring supports tend to be overloaded. The aim of this section is to estimate the overload.

In the presented results, the damage level is represented by a decrease in the support dynamic stiffness. More precisely, the dynamic stiffness of the two elastic stages of the damaged support is multiplied by a coefficient lower than one. This choice is justified by the low stiffness of the elastic stages compared to the other components in the studied track. This choice also eases the comparison between both models.

Five levels of degradation of the damaged support are considered: 0% – healthy track –, 25%, 50%, 75% et 99% – almost completely broken support. For both methods, the computation is made with a maximal frequency of $300\,\text{Hz}$ and a $1\,\text{Hz}$ frequency step.

In the numerical model, the rail, the reinforced concrete block, the two elastic pads and the underlying concrete slab are finely modeled in three dimensions. The used geometry and mesh are represented in figure 4. The same mesh is used in the three zones. Only the stiffness of each elastic pad is changed in the transition zone.
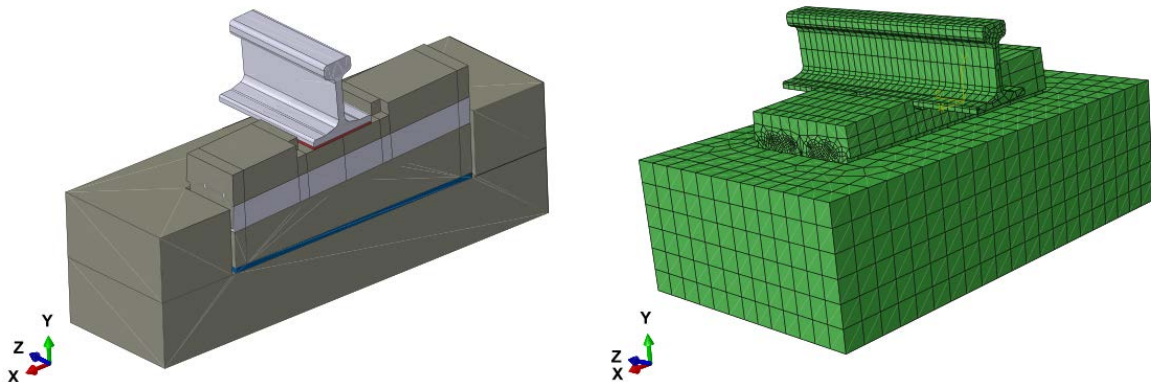

Figure 4: Cross-sectional view of the geometry and mesh of one pattern.

The parameters used to describe the tracks in the analytical and numerical models are given in table 1.

3.1 Analytical results

In this computation, the damaged support is numbered support 0. In Figure 5, the maximal force applied on each support is plotted against the support number for the different damage states of support 0. As expected, the more the central support is damaged, the more the neighboring supports are loaded. In every case, the overload is mainly distributed to supports -1 and $+1$.

Table 2 gives the maximum force applied on supports -2 to 2 and on support 20 which is supposed to be far enough from the damage to be independent of the damage level. These results are given for the different damage levels of the damaged support. The small asymmetry between supports before and after the damaged one is due to damping in the under-sleeper and under-rail pads.

Parameter	Value
Steel density	$7.8\,\mathrm{kg/dm^3}$
Steel Young modulus	$210\,\mathrm{GPa}$
Rail inertia	$3.038 \times 10^{-5}\,\mathrm{m^4}$
Timoshenko coefficient	0.4
Rail section	$7.64 \times 10^{-3}\,\mathrm{m^3}$
Shear modulus	$8.077\,\mathrm{GPa}$
Train speed	$37\,\mathrm{m \cdot s^{-1}}$
Support spacing	$0.6\,\mathrm{m}$
Concrete Young modulus	$50\,\mathrm{GPa}$
Concrete density	$2.4\,\mathrm{kg/dm^3}$
Under-rail pad Young modulus	$20\,\mathrm{MPa}$
Under-rail pad stiffness	$192\,\mathrm{MN \cdot m^{-1}}$
Under-rail pad density	$1\,\mathrm{kg/dm^3}$
Under-rail pad dampening	$1.97\,\mathrm{MN \cdot s \cdot m^{-1}}$
Under-sleeper pad Young modulus	$20\,\mathrm{MPa}$
Under-sleeper pad stiffness	$26.4\,\mathrm{MN \cdot m^{-1}}$
Under-sleeper pad density	$1\,\mathrm{kg/dm^3}$
Under-sleeper pad dampening	$0.17\,\mathrm{MN \cdot s \cdot m^{-1}}$

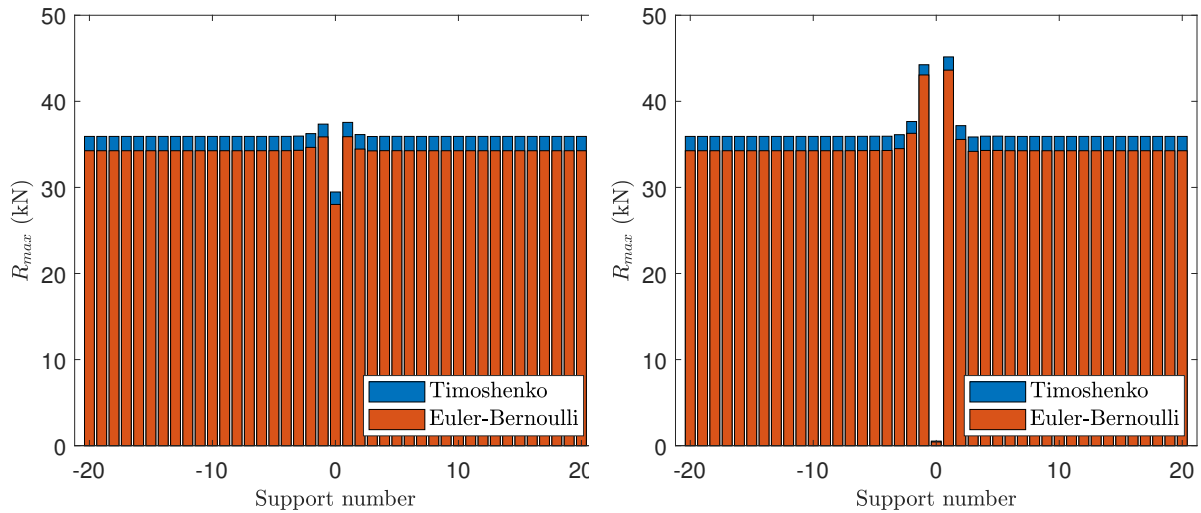Table 1: Mechanical parameters of the track components.

Figure 5: Maximum load applied on each support for a damage level of 0.25 (left) and 0.99 (right).

3.2 Numerical results

The numerical method developed by Claudet *et al.* [16] gives access to the displacements at every nodes in the mesh. These displacements are numerically derived to compute the strains in each element. Then, using Hooke law, the stress tensor is computed. Finally, this stress is used to compute a failure criterion in every element of the mesh. As the concrete has different strengths in tension σ_t and compression σ_c, the Drucker-Prager yield criterion was chosen. This

Damage level	Support number					
	-2	-1	0	1	2	20
0	36.1	36.1	36.1	36.1	36.1	36.1
0.25	36.5	37.6	29.7	37.7	36.3	36.1
0.50	36.9	39.4	21.8	39.7	36.6	36.1
0.75	37.4	41.5	12	42.1	36.9	36.1
0.99	37.9	44.5	0.5	45.3	37.2	36.1

Table 2: Maximal loads (kN) applied on each support in function of the damage level.

criterion can be expressed as follows:

$$C = \left(\sqrt{3J_2} - BI_1 \right) /A \tag{15}$$

Where J_2 and I_1 are the usual stress tensor invariants and A and B are defined by:

$$\begin{aligned} A &= 2\frac{\sigma_c \sigma_t}{\sigma_c + \sigma_t} \\ B &= \frac{\sigma_t - \sigma_c}{\sigma_c + \sigma_t} \end{aligned} \tag{16}$$

This failure criterion compares the stress computed in each element to the strenghts of their constitutive material. A value of 1 means the material will experience plastic yield in one cycle.
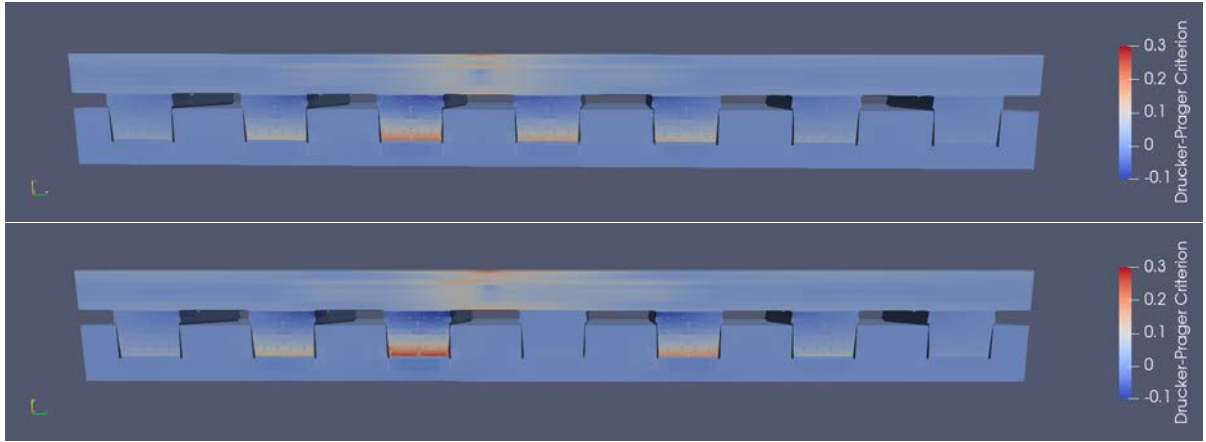

Figure 6: Drucker-Prager failure criterion at $t = 0$ for a damage level of 0.25 (top) and of 0.99 (bottom).

Figure 6 gives a cutted view of the computed Drucker-Prager criterion at $t = 0$ for different damage levels of the damaged support. The localization of the maximum of this criterion shows a strong agreement with damages observed in real track supports. As expected, more loaded supports experience a higher Drucker-Prager criterion. This phenomenon can lead to early fatigue damage and, therefore, damages propagation along the track.

As previously, we numbered the different supports with number 0 corresponding to the damaged support. Table 3 gives the maximum value of the Drucker-Prager criterion in function of the support number and the damage level of the damaged support. Once again, the overload seems to be mainly supported by the two closest supports. This overload grows with the damage level.

Damage level	Support number						
	-3	-2	-1	0	1	2	3
0	0.173	0.173	0.174	0.173	0.174	0.173	0.173
0.25	0.173	0.175	0.181	0.141	0.182	0.175	0.173
0.5	0.173	0.177	0.191	0.103	0.192	0.177	0.173
0.75	0.173	0.179	0.204	0.057	0.204	0.179	0.174
0.99	0.173	0.182	0.219	0.004	0.221	0.182	0.174

Table 3: Maximum value of Drucker-Prager criterion in function of support number and damage level.

3.3 Comparison of the results given by the two methods

The analytical method allows a rapid computation of the maximal force applied on each support. On the other hand, with a much higher cost, the numerical can give access to the Drucker-Prager failure criterion at components scale. In Figure 7, the maxima of Drucker-Prager failure criterion for each support are plotted in function of the maxima of forces computed with the analytical model. These two values show a strong linear correlation with a regression coefficient $R^2 = 0,998$. This result proves that, in the case a a track containing a single damaged support, the analytical method can be a good method with low cost to assess the stresses in the supports.
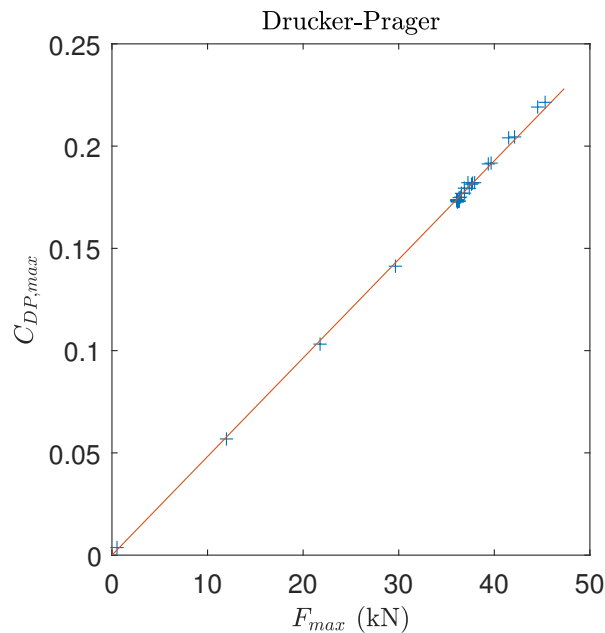

Figure 7: Temporal maximum Drucker-Prager failure criteria computed with the numerical method in function of maximum loads computed with the analytical one. Results and linear regression.

4 Conclusion

In this article, we studied the load level of the different supports in a ballastless railway track containing one damaged support. To compute these load levels, two different methods were used. The first one is based on a very simplified representation of the track whose response is computed analytically. Being analytical, this method allows very quick computation of the

Benjamin Claudet, Denis Duhamel, Gilles Foret, Tien Hoang, Francis Sabatier, Bertrand Findinier, and Hervé Lenglin

track behavior. To access finer results – such as stresses and strains at the component scale – we used a numerical method. With this method, the use of a fine three-dimensional representation of the track implies a much higher numerical cost.

With the numerical method, the Drucker-Prager failure criterion was computed at the component scale with a three-dimensional geometry. The localization of the maxima of this criterion was in strong agreement with the damages observed in real tracks.

In the final section, the analytical results were compared with the numerical ones. We found that the maximum loads per support analytically computed are in strong linear correlation with the maximum Drucker-Prager criterion numerically computed. This correlation demonstrates the analytical method's usefulness in providing a quick assessment of stresses in the different materials of the supports.

References

[1] P.M. Belotserkovskiy. "On The Oscillation of infinite periodic beams subjected to a moving concentrated force". In: *Journal of Sound and Vibration* 193.3 (June 1996), pp. 705–712. ISSN: 0022-460X. DOI: 10.1006/JSVI.1996.0309. URL: https://www.sciencedirect.com/science/article/pii/S0022460X96903090.

[2] A. Nordborg. "Vertical Rail Vibrations: Parametric Excitation". In: *ACUSTICA· acta acustica* 84 (1998), pp. 289–300. URL: http://www.soundview.de/wp-content/uploads/2015/04/A-Nordborg-Vertical-Rail-Vibrations-Parametric-Excitation.pdf.

[3] T. Hoang et al. "Calculation of force distribution for a periodically supported beam subjected to moving loads". In: *Journal of Sound and Vibration* 388 (Feb. 2017), pp. 327–338. ISSN: 10958568. DOI: 10.1016/j.jsv.2016.10.031. URL: http://dx.doi.org/10.1016/j.jsv.2016.10.031%20https://www.sciencedirect.com/science/article/pii/S0022460X1630565X.

[4] T. Hoang, D. Duhamel, and G. Foret. "Dynamical response of a Timoshenko beams on periodical nonlinear supports subjected to moving forces". In: *Engineering Structures* 176 (Dec. 2018), pp. 673–680. ISSN: 0141-0296. DOI: 10.1016/J.ENGSTRUCT.2018.09.028. URL: https://www.sciencedirect.com/science/article/pii/S014102961832995X.

[5] Elodie Arlaud, S Costa D'aguiar, and E Balmes. "Receptance of railway tracks at low frequency: Numerical and experimental approaches". In: *Transportation Geotechnics* 9 (2016), pp. 1–16. DOI: 10.1016/j.trgeo.2016.06.003. URL: http://dx.doi.org/10.1016/j.trgeo.2016.06.003.

[6] T. Hoang et al. "Wave finite element method for the dynamic analysis of railway tracks". In: *13th World Congress on Computational Mechanics (WCCM XIII) 2nd Pan American Congress on Computational Mechanics (PANACM II)*. New York City, NY, USA, 2018.

[7] Xianying Zhang, David Thompson, and Xiaozhen Sheng. "Differences between Euler-Bernoulli and Timoshenko beam formulations for calculating the effects of moving loads on a periodically supported beam". In: *Journal of Sound and Vibration* 481 (2020), p. 115432. ISSN: 10958568. DOI: 10.1016/j.jsv.2020.115432. URL: https://doi.org/10.1016/j.jsv.2020.115432.

[8] B Claudet et al. "Application of the Wave Finite Element method to the computation of the response of a ballastless railway track, comparison with on-site measurements". In: *Proceedings of The Fifth International Conference on Railway Technology: Research,*

Development and Maintenance. Ed. by J. Pombo. Vol. 1. Civil-Comp Press, Edinburgh, UK, 2022. DOI: `10.4203/ccc.1.8.1`.

[9] T. Hoang et al. "Computational method for the dynamics of railway tracks on a non-uniform viscoelastic foundation". In: *Procedia Engineering*. Vol. 199. 2017, pp. 354–359. DOI: `10.1016/j.proeng.2017.09.034`. URL: `www.sciencedirect.comwww.sciencedirect.com`.

[10] Le-hung Tran et al. "Calculation of the dynamic responses of a railway track on a non-uniform foundation". In: *Journal of Vibration and Control* May (May 2022), p. 107754632210993. ISSN: 1077-5463. DOI: `10.1177/10775463221099353`. URL: `http://journals.sagepub.com/doi/10.1177/10775463221099353`.

[11] Benjamin Claudet et al. "A comparison of beam models for the dynamics of railway tracks on a non-uniform viscoelastic foundation". In: *ICSV2021*. 2021, pp. 1–8.

[12] Mojtaba Shahraki, Chanaka Warnakulasooriya, and Karl Josef Witt. "Numerical study of transition zone between ballasted and ballastless railway track". In: *Transportation Geotechnics* 3 (2015). ISSN: 22143912. DOI: `10.1016/j.trgeo.2015.05.001`. URL: `http://dx.doi.org/10.1016/j.trgeo.2015.05.001`.

[13] José Nuno Varandas, Paul Hölscher, and M. A.G. Silva. "Three-dimensional track-ballast interaction model for the study of a culvert transition". In: *Soil Dynamics and Earthquake Engineering* (2016). ISSN: 02677261. DOI: `10.1016/j.soildyn.2016.07.013`.

[14] T Gras et al. "On a coupling between the Finite Element (FE) and the Wave Finite Element (WFE) method to study the effect of a local heterogeneity within a railway track". In: *Journal of Sound and Vibration* 429 (2018), pp. 45–62. ISSN: 10958568. DOI: `10.1016/j.jsv.2018.05.011`. URL: `https://doi.org/10.1016/j.jsv.2018.05.011`.

[15] André Paixão et al. "Numerical simulations to improve the use of under sleeper pads at transition zones to railway bridges". In: *Engineering Structures* 164 (June 2018), pp. 169–182. ISSN: 0141-0296. DOI: `10.1016/J.ENGSTRUCT.2018.03.005`. URL: `https://www.sciencedirect.com/science/article/pii/S014102961733078X?via%3Dihub`.

[16] Benjamin Claudet et al. "Wave Finite Element Method for Computing the Dynamic Response of Railway Transition Zones". In: *Proceedings of the 7th International Conference on Computational Methods in Structural Dynamics and Earthquake Engineering (COMPDYN 2015)*. Vol. 3. Crete, Greece: Institute of Structural Analysis and Antiseismic Research School of Civil Engineering National Technical University of Athens (NTUA) Greece, 2019, pp. 4538–4547. ISBN: 978-618-82844-5-6. DOI: `10.7712/120119.7247.18688`. URL: `www.eccomasproceedia.org%20https://www.eccomasproceedia.org/conferences/thematic-conferences/compdyn-2019/7247`.

[17] T. Hoang et al. "Wave finite element method for vibration of periodic structures subjected to external loads". In: *6th European Conference on Computational Mechanics (ECCM 6)*. June. 2018, pp. 11–15. URL: `http://www.eccm-ecfd2018.org/admin/files/filePaper/p218.pdf`.